

Behavior of Sulfonated Poly(ether ether ketone) in Ethanol–Water Systems

Kimball S. Roelofs, Andreas Kampa, Thomas Hirth, Thomas Schiestel

Fraunhofer Institute for Interfacial Engineering and Biotechnology, Nobelstraße 12, 70569 Stuttgart, Germany

Received 8 May 2008; accepted 8 August 2008

DOI 10.1002/app.29351

Published online 5 December 2008 in Wiley InterScience (www.interscience.wiley.com).

ABSTRACT: The behavior of sulfonated poly(ether ether ketone) (sPEEK) membranes in ethanol–water systems was studied for possible application in direct ethanol fuel cells (DEFCs). Polymer membranes with different degrees of sulfonation were tested by means of uptake, swelling, and ethanol transport with dynamic measurements (liquid–liquid and liquid–gas systems). Ethanol permeability was determined in an liquid–liquid diffusion cell. For membranes with an ion-exchange capacity (IEC) between 1.15 and 1.75 mmol/g, the ethanol permeability varied between 5×10^{-8} and 1×10^{-6} cm²/s, being dependent on the measuring temperature. Ethanol and water transport in liquid–gas systems was tested with pervaporation as a function of IEC and temperature. Higher IEC accounted for higher fluxes and lower water/ethanol selectivity. The temperature had a large effect on the fluxes, but the selectivity remained constant. Further-

more, the membranes were characterized with proton conductivity measurements. The proton diffusion coefficient was calculated, and a transition in the proton transfer mechanism was found at a water number of 12. Membranes with high IEC (>1.6 mmol/g) exhibited larger proton diffusion coefficients in ethanol–water systems than in water systems. The membrane with the lowest IEC exhibited the best proton transport to ethanol permeability selectivity. The use of sPEEK membranes in DEFC systems depends on possible modifications to stabilize the membranes in the higher conductive region rather than on modifications to increase the proton conductivity in the stable region. © 2008 Wiley Periodicals, Inc. *J Appl Polym Sci* 111: 2998–3009, 2009

Key words: diffusion; ionomers; membranes; poly(ether ketones); swelling

INTRODUCTION

Poly(ether ether ketone) (PEEK) is a broadly applied polymer because of its high mechanical, thermal, and chemical resistance and low cost. The easy modification of the hydrophobic polymer chain by sulfonation accounts for the easy adjustment of hydrophilic and hydrophobic regions. This feature, combined with the stability characteristics, makes sulfonated poly(ether ether ketone) (sPEEK) highly interesting for membrane technology. Possible applications can be found in pervaporation,^{1,2} gas dehydration,^{3,4} and various ion-exchange processes.⁵ In the last category, the application of sPEEK as a polymer electrolyte membrane in fuel cells has been widely studied.^{6–9} In the case of direct alcohol fuel cells, many studies have been carried out on methanol as a fuel in so-called direct methanol fuel

cells.^{8,10,11} Here sPEEK has been used to prepare pure polymer membranes^{12–14} and polymer blend membranes^{15,16} or as a polymer matrix in organic–inorganic composite membranes.^{17–20} Only a couple of studies are known for direct ethanol fuel cells (DEFCs).^{21,22} Ethanol has some evident advantages over methanol, such as environmental compatibility, lower toxicity, and an existing infrastructure for distribution. Moreover, ethanol contains a higher energy density than methanol, and it is a generally known and accepted chemical.

In this article, we describe the preparation of sPEEK membranes and the behavior of these proton-conductive membranes in aqueous–ethanolic environments. The degree of sulfonation (DS) was varied by the regulation of the sulfonation temperature. The proton-conducting properties of the membranes were investigated with impedance spectroscopy in water and water–ethanol systems. The swelling behavior in water and aqueous–ethanolic environments was studied at room temperature (RT). The stability at temperatures up to 80°C was tested in water. Ethanol transport through the membranes was studied in liquid–liquid (L–L) and liquid–gas (L–G) systems (L–L diffusion and pervaporation, respectively).

Correspondence to: T. Schiestel (thomas.schiestel@igb.fraunhofer.de).

Contract grant sponsor: Fraunhofer Organization (within the Fraunhofer project “Direct Ethanol Fuel Cells”; see www.defc.de).

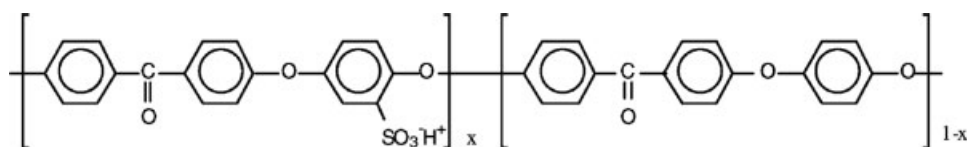


Figure 1 Repeat units of sPEEK ($x \times 100\% = \text{DS}$).

EXPERIMENTAL

Chemicals

PEEK (450G) was obtained from Victrex (Thornton Cleveleys, Lancashire, UK) and sulfuric acid (95–97%) was obtained from Sigma Aldrich (Buchs, Switzerland). Sodium chloride (NaCl) and sodium hydroxide (NaOH) were both obtained from Merck (Darmstadt, Germany), *N*-methyl-2-pyrrolidone (NMP; 99.8%) and hydrochloric acid (HCl; 25%) were obtained from Roth (Karlsruhe, Germany), and ethanol (>99.8%) was obtained from AppliChem (Darmstadt, Germany). All chemicals were used as received without further purification.

Sulfonation of PEEK

The sulfonation of PEEK was performed similarly to the procedures reported in the literature.^{23,24} The sulfonation was carried out in a 1-L jacketed flat-bottom flask fitted with a mechanical stirrer. PEEK was dissolved in sulfuric acid for 16 h at RT. Then, the solution was heated to a certain temperature between 35 and 60°C and kept at that temperature for 5 h. The solution was cooled below 15°C in 45 min to arrest the reaction. The viscous solution was quenched in ice water and washed several times until the pH was higher than 6. The polymer was wrung out and transferred into a 60°C drying oven for 6 h. After that, the polymer was transferred to a vacuum oven (80°C/<100 mbar) for 20 h. The chemical structure of sPEEK is presented in Figure 1.

Membrane preparation

A polymer solution was prepared by the dissolution of 3 g of sPEEK in 25 mL of NMP. The solution was stirred at RT for 3 days. In the case of poorly dissolving polymers (low DS), the solution was heated to 120°C for 3 h. Polymer membranes were prepared by a casting and solvent evaporation process.¹⁸ Before casting, a glass plate was cleaned with NMP followed by acetone. Then, a film of the polymer solution was cast with a 0.6-mm doctor blade. The solvent was evaporated by drying in an oven at 70°C for 20 h followed by drying in a vacuum oven (100°C/<100 mbar) for 20 h. The membranes, which adhered to the glass plates, were soaked in a deionized (DI) water bath for 2 h. After

that, the membranes were peeled off from the glass plate. Protonation was carried out in 1M HCl for 1.5 h and was followed by soaking of the membranes again in DI water for 2 h. The membranes were air-dried and stored until further characterization. The thickness of the membranes varied between 30 and 40 μm .

Membrane characterization

DS and ion-exchange capacity (IEC)

DS of the polymers and membranes was determined by titration. In addition, DS of the polymers was measured by NMR.

Titration. About 0.2 g of polymer per membrane was freshly protonated in 1M HCl for 20 h. Then, the membranes were rinsed extensively with DI water. After that, the membranes were air-dried; this was followed by drying in a vacuum oven (80°C/<100 mbar/16–20 h). The dry weight was determined before the transfer of the membranes into 2M NaCl and stirring for 20 h to exchange the protons with the sodium cations. Back-titration was performed with 0.05M NaOH automatically with a titroprocessor (Metrohm, Filderstadt, Germany).

IEC is defined as follows:

$$\text{IEC} = \frac{\text{Ion exchange active groups}}{\text{Dry mass of the membrane}} \quad (1)$$

In the case of polymer membranes, DS (defined between 0 and 1) can be calculated as follows^{23,25}:

$$\text{DS} = \frac{M_{w,p} \text{IEC}}{1 - M_{w,f} \text{IEC}} \quad (2)$$

where $M_{w,p}$ is the molecular weight of the nonfunctional polymer repeat unit and $M_{w,f}$ is the molecular weight of the functional group with the counter ion ($-\text{SO}_3\text{H}$).

¹H-NMR. ¹H-NMR spectroscopy was used to quantify the sulfonic acid groups in the copolymer. The presence of the sulfonic acid groups accounts for a significant downfield shift of the proton on the position next to this group. The fundamentals of the characterization of sulfonated polymers by NMR is given by Nolte et al.²⁶ This technique is nowadays a common method for verifying DS.^{14,23,24,27} The equation for determining DS from the integrals of the NMR peaks is:

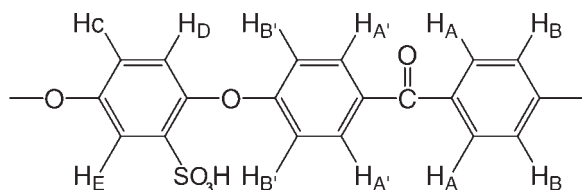


Figure 2 Nomenclature of the aromatic protons for the sPEEK repeat unit.

$$\frac{DS}{12 - 2DS} = \frac{AH_E}{\sum AH_{A,A',B,B',C,D}} \quad (3)$$

The nomenclature of the aromatic protons is given in Figure 2. The $^1\text{H-NMR}$ spectra were recorded on a Bruker Advance DPX 250 NMR spectrometer (Bruker, Rheinstetten, Germany) at a resonance frequency of 250.13 MHz. Polymer solutions (between 0.5 and 5%) were prepared in hexadeuterated dimethyl sulfoxide, and tetramethylsilane was used as the internal standard.

Uptake and swelling degree

The determination of the uptake and swelling degree of the surface area ($SD_{\text{surface area}}$) was performed in water and 2M ethanol at RT. The diameter of the membrane samples was 25 mm. The dry weight and diameter were determined after a drying procedure ($80^\circ\text{C}/<100$ mbar/16–20 h) before the measurements. The wet diameter (d_{wet}) and wet weight (m_{wet}) were measured until they were constant (6–12 days). d_{wet} was determined directly after the membrane was taken out of the liquid. m_{wet} was determined after the removal of the surface liquid by the placement of the membrane between dust-free cloths and gentle pressing with 28.5 N cm^2 . Afterwards, the dry weight and diameter were determined again to see if there were any irreversible changes.

The water and 2M ethanol uptake and $SD_{\text{surface area}}$ values of the membranes were calculated as follows:

$$\text{Uptake} = \frac{m_{\text{wet}} - m_{\text{dry}}}{m_{\text{dry}}} \cdot 100\% \quad (4)$$

$$SD_{\text{surface area}} = \frac{\frac{\pi}{4}d_{\text{wet}}^2 - \frac{\pi}{4}d_{\text{dry}}^2}{\frac{\pi}{4}d_{\text{dry}}^2} \cdot 100\% \quad (5)$$

The swelling degree of the membranes in water was also determined at various temperatures. The diameter of the samples was 16 mm. The membranes were dried overnight in a vacuum oven at 80°C . The diameter of the dried samples (d_{dry}) was

determined, and this was followed by soaking of the membranes for 45 min in water at different temperatures: 40, 50, 60, 70, and 80°C . The diameter of the swollen membranes (d_{wet}) was measured, and with eq. (5), $SD_{\text{surface area}}$ was calculated.

Sorption behavior

Sorption experiments were performed to determine the equilibrium concentration of water and ethanol in the membrane. The experiment was similar to that described in the literature.^{1,28} Membrane samples of 1.5–3 g (depending on the IEC of the membranes) were immersed in 2M ethanol for 1 day. The sample was taken out of the liquid, and surface liquid was removed as previously described. The membrane was placed in a glass tube, and desorption *in vacuo* was performed. The evaporated gas was collected in a cold trap in liquid nitrogen. The mass of the sample was compared to the mass decrease of the membrane sample. The composition of the sample was determined with a refractometer (DR301-95, A. Krüss Optronic, Hamburg, Germany).

The sorption selectivity was determined as follows:

$$\text{Sorption selectivity} = \frac{m_{i, \text{membrane}}/m_{j, \text{membrane}}}{m_{i, \text{sorption liquid}}/m_{j, \text{sorption liquid}}}$$

where m is the mass fraction of component i or j in the desorbed liquid and the initial ethanol–water mixture (indicated by the subscripts *membrane* and *sorption liquid*, respectively).

Proton conductivity

The proton conductivity was measured by alternating-current impedance spectroscopy with an electrochemical workstation (IM6, Zahner, Kronach, Germany). The measurements were carried out in the potentiostatic mode over the frequency range of 1–1000 Hz with an oscillating voltage of 5 mV.

Two different setups were used to determine the proton conductivity in the longitudinal direction at RT in the wet state. The spring tip configuration (STC) consisted of four spring tip electrodes (spring probes; P19-2221, Harwin, Portsmouth, UK; Fig. 3, right).^{29–31} In this case, circular membranes with a diameter of 25 mm were used. The platinum wire configuration (PWC) was based on the setup proposed by Zadowzinski et al.³² and also used, for example, in refs. 33 and 34. The setup consisted of four platinum wires (diameter = 0.5 mm) with a 15-mm length and a 17-mm distance between them (Fig. 3, left). In that case, the dimensions of the

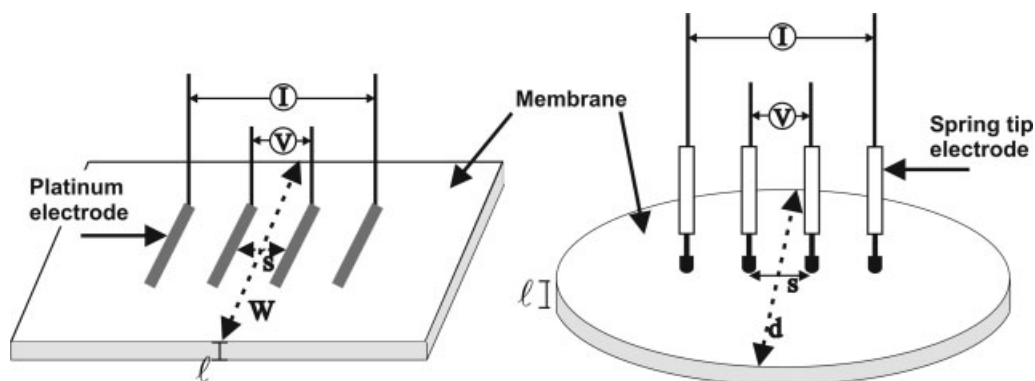


Figure 3 Schematic representation of the PWC (left) and the STC (right).

membrane samples were 50 mm × 100 mm. The electrodes were pressed onto the membranes with 2 kg/cm². In all cases, the membranes were pretreated in 1M HCl for 20 h, and this was followed by extensive rinsing with DI water. After that, the membranes remained in DI water or 2M ethanol for at least 20 h before the measurements were performed.

The proton conductivity for the STC [$\sigma(\text{STC})$] and the PWC [$\sigma(\text{PWC})$] was calculated as follows^{30,33}:

$$\sigma(\text{STC}) = \frac{\ln 2}{\pi} \frac{1}{\ell \cdot |Z|_{-2^\circ < \varphi < 2^\circ}} \cdot \frac{1}{f_1 \cdot f_2} \quad \text{and} \quad (6)$$

$$\sigma(\text{PWC}) = \frac{s}{|Z|_{-2^\circ < \varphi < 2^\circ} \cdot W \cdot \ell}$$

where ℓ is the membrane thickness; $|Z|_{-2^\circ < \varphi < 2^\circ}$ is the average impedance; correction factors f_1 and f_2 are the finite thickness and the finite width correction, respectively; W is the width of the membrane sample; and s is the distance between the inner electrodes. The conductivity determined with the STC is dependent on ℓ and $|Z|_{-2^\circ < \varphi < 2^\circ}$. The latter is the average impedance of three frequency series in which the phase is between -2 and 2° .³¹ In this area, it was assumed that the impedance equals the

membrane resistance. In the case of the PWC, the conductivity is also dependent on W and s .

Ethanol permeability

L-L systems. Ethanol permeability was determined in a diffusion cell, as shown in Figure 4. The cell consisted of a water compartment (1) and an ethanol compartment (2). The membrane (3) was placed between two perforated metal supports (5) and was sealed with O-rings (4). The effective membrane surface was 14.7 cm². Both compartments were stirred magnetically to provide agitation. A pipette (6) was placed on the water compartment to monitor the volume change during time interval Δt . A syringe (7) was used to collect samples of 0.3 mL. In the ethanol compartment, the ethanol solution was circulated by means of a pump (8) to ensure a constant concentration on the ethanol side. The temperature of the supply (9; ~ 400 mL) was regulated with a water bath (10). Heating channels in the diffusion cell were connected to the water bath to ensure a constant temperature in the whole system.

Besides the ethanol permeability, the water permeability was also determined. The flux directions,

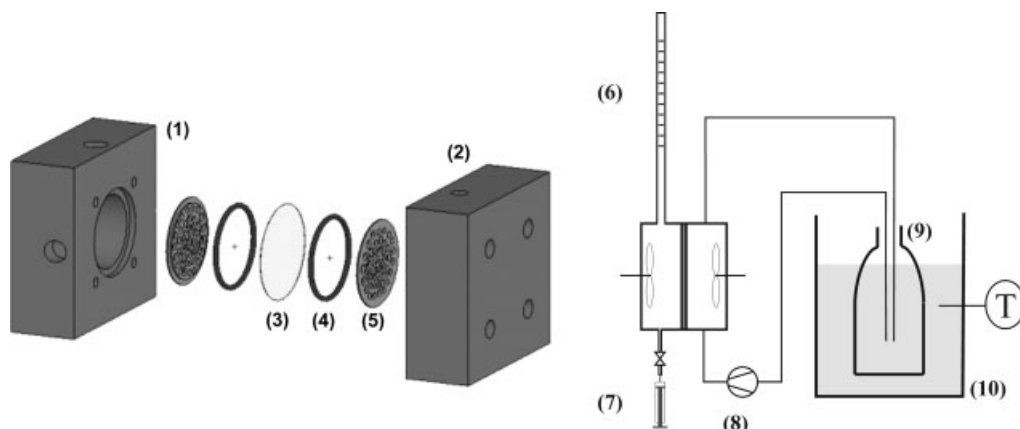


Figure 4 Schematic representation of the diffusion cell (left) and the setup (right).

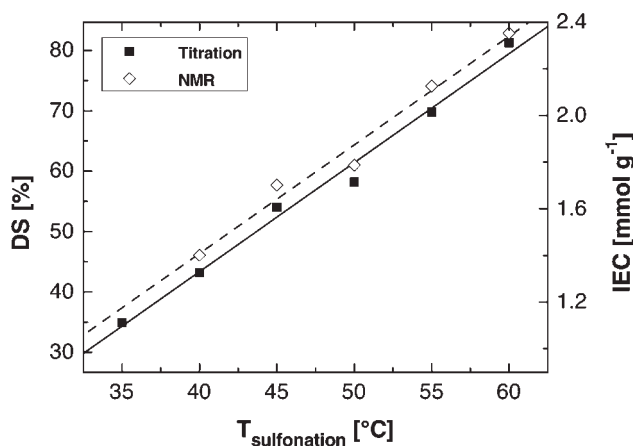


Figure 5 IEC and DS as functions of the sulfonation temperature ($T_{\text{sulfonation}}$) determined by titration and $^1\text{H-NMR}$.

however, were in opposite directions. The permeability coefficients of ethanol (P_{EtOH}) and water (P_{water}) were determined based on Fick's diffusion equation:

$$J_{\text{EtOH}} = \frac{\Delta n_{\text{EtOH}}}{A \cdot \Delta t} = P_{\text{EtOH}} \frac{C_{\text{EtOH},E} - C_{\text{EtOH},W}}{\ell} \quad (7)$$

$$J_{\text{water}} = \frac{\Delta n_{\text{water}}}{A \cdot \Delta t} = P_{\text{water}} \frac{C_{\text{water},W} - C_{\text{water},E}}{\ell} \quad (8)$$

where J_{EtOH} is the flux of ethanol; J_{water} is the flux of water; $C_{\text{EtOH},E}$ and $C_{\text{EtOH},W}$ are the concentrations of ethanol in the ethanol and water compartments, respectively; $C_{\text{water},E}$ and $C_{\text{water},W}$ are the concentrations of water in the ethanol and water compartments, respectively; Δn_{EtOH} and Δn_{water} are the molar amounts of ethanol resp. water permeated through the membrane in time interval Δt ; and ℓ and A are the membrane thickness and surface area, respectively. Before testing, the membranes were pretreated in a 4M ethanol solution for at least 16 h. $C_{\text{EtOH},E}$ was 4M and was assumed to be constant during the measurement because of the 10 times larger volume in comparison with the water side (concentration decline < 7.5%). The ethanol concentration was determined with a refractometer, and the measurements were performed at 25, 40, 50, and 60°C.

L-G systems. A circular membrane with an area of 40.7 cm² was built into a pervaporation cell. The membrane was put on a sintered metal support (pore size = 10 μm) and sealed with O-rings. The membrane was pretreated for at least 16 h in an ethanol solution with the same molarity used with the measurement. During the measurement, the temperature on the feed side was kept constant by the connection of a water bath to the cell. Measurements were performed between 25 and 70°C. The permeate pressure was maintained at 10–15 mbar, and the permeate was condensed with liquid nitrogen in a

glass cold trap. The permeate was weighed, and the ethanol concentration was determined with a refractometer. The measurements were started after 1.5 h of conditioning, and at least four measuring points were taken for building the average permeation rate and selectivity. The selectivity is expressed in terms of the separation factor. This is a process parameter and indicates the overall selectivity of the whole measurement system. The permeation rate (J) and separation factor (α) were calculated as follows:

$$J = \frac{w\ell}{A\Delta t} \quad \text{and} \quad \alpha = \frac{y_i/y_j}{x_i/x_j} \quad (9)$$

where w is the weight of the permeate collected in time interval Δt and x and y are the molar fractions in the feed and permeate of components i and j .^{1,2,19}

RESULTS AND DISCUSSION

DS and IEC

DS and IEC as functions of the sulfonation temperature are shown in Figure 5. There is a linear relationship in that temperature interval, and DS can be well controlled or predicted. In all cases, the values measured by NMR are slightly higher. With a different titration method, Huang et al.²³ determined values that are consistent with our results. It is remarkable that they also observed a constant difference between both methods, but in all cases the titration values were slightly higher. For all further calculations, the titration values were taken.

Uptake, swelling degree, and sorption

The uptake and swelling of the polymer membranes as a function of IEC are given in Figure 6. Both the uptake and swelling increase exponentially with increasing IEC, so the uptake and swelling of the membranes in 2M ethanol always exceed the water values. Up to an IEC of 1.6 mmol/g, the differences are below 20%. Considerably higher uptake and swelling in 2M ethanol in comparison with water can be observed when IEC exceeds this value. The increase of IEC implies an increase of hydrophilicity. More liquid is absorbed, and therefore the polymer structure swells. For shorter storage times (<1 day), Li et al.¹² found a linear increase for the water uptake as a function of IEC up to an IEC of 2.0 mmol/g followed by a rapid increase in the water uptake with higher IEC. This increase was also observed by Xue and Yin¹⁴ but started at 1.76 mmol/g. In this range of IECs, a shift can be observed in the hydrophobicity–hydrophilicity balance. The hydrophobic regions, which ensure stability, are separated by the hydrophilic regions. The

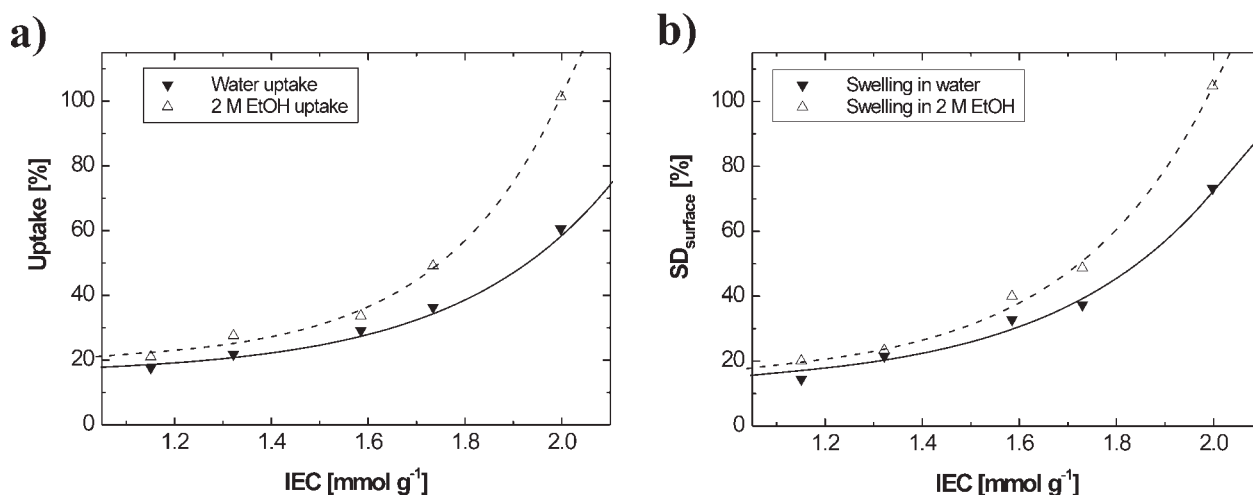


Figure 6 (a) Water and 2M ethanol uptake and (b) swelling as functions of IEC.

further increase in the amount of water occurs as a second phase³⁵ resulting in excessive swelling. In our work, this behavior is more pronounced in ethanol solutions.

The uptake after 1 day of immersion was also verified. For all membranes with an IEC lower than 2 mmol/g, the uptake deviation between 1 and 12 days is below 3.5%. The deviation for the higher sulfonated membrane is larger (7.2%). The application of the latter material is less relevant because of the extreme structural changes under the tested conditions. This short time was chosen to precondition the membrane for other characterization methods such as proton conductivity and ethanol permeability measurements.

A parameter that to some extent describes the hydrophilicity is the water number. The water number (λ_{water}) is the ratio of the molar amount of water (n_{water}) to the molar amount of sulfonic acid groups present in the membrane ($n_{\text{-SO}_3\text{H}}$):

$$\lambda_{\text{water}} = \frac{n_{\text{water}}}{n_{\text{-SO}_3\text{H}}} = \frac{\text{Uptake}}{\text{IEC} \cdot M_{w,\text{water}}} \quad (10)$$

In this case, the defined uptake is dimensionless, and $M_{w,\text{water}}$ is the molar mass of water. Similar to the water number determined with eq. (10), the water and ethanol numbers can be calculated on the basis of the 2M ethanol uptake and the ethanol concentration in the membrane. This concentration is determined with sorption experiments, which were also described by Huang et al.¹ for isopropyl alcohol and water in sPEEK membranes. In Figure 7, the decrease in the sorption selectivity as a function of IEC is shown. It is remarkable that under similar conditions, Huang et al. found a constant and significantly higher sorption selectivity (4) in a similar IEC range. These different findings result from the differ-

ence in the solubility of ethanol and isopropyl alcohol in water.

The molar ratios of water and ethanol to the sulfonic acid groups (λ'_{water} and λ'_{EtOH} , respectively) are given in Figure 8. Up to an IEC of 1.6 mmol/g, both λ'_{water} and λ'_{EtOH} are relatively constant. The water numbers in the ethanol–water system are in all cases higher than the water numbers in the pure water system. Above the IEC of 1.6 mmol/g, the increase in the ethanol and water numbers is more pronounced as the water number in the pure water system. The difference between the two water numbers increases at higher IEC. The water uptake and the structural deformation of the membrane are affected by ethanol present in the membrane in the static measurements and are also expected to affect the fluxes in the dynamic measurements.

The surface swelling in water as a function of temperature is given in Figure 9. The swelling increases with temperature. The membrane with an IEC of 1.15 mmol/g was just slightly deformed in the

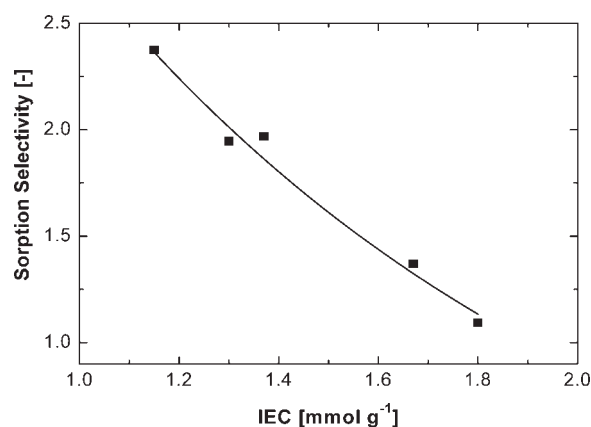


Figure 7 Sorption selectivity as a function of IEC.

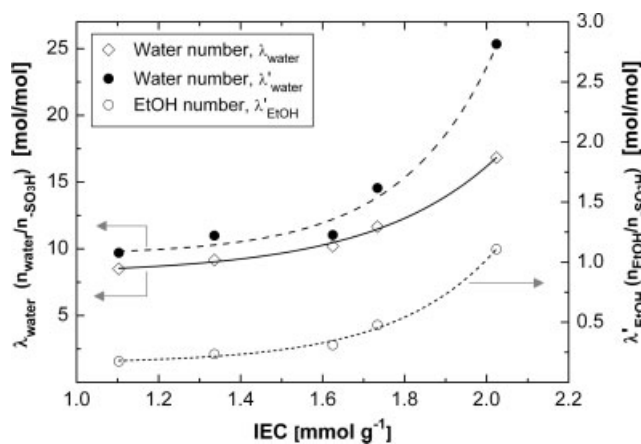


Figure 8 Water numbers determined from the water and 2M ethanol uptake (λ_{water} and λ'_{water} respectively) and ethanol number (λ'_{EtOH}).

temperature range. The membranes with high IEC (>1.7 mmol/g) swelled excessively, so at higher temperatures, it was impossible to measure the swelling because of the fragile structure of the membrane or partial dissolution in the heated liquid.

Proton conductivity

Proton conductivity was measured with two different in-plane configurations to obtain information about the reliability of the measurements. The proton conductivity in water measured with the PWC was almost identical to the values measured with the STC. The proton conductivity measured with the STC of sPEEK membranes with various IECs wetted in water and 2M ethanol is given in Figure 10. In the region in which the uptake in water and 2M ethanol remains low (<1.6 mmol/g), the proton conductivity in both systems is similar. From that point, the proton conductivity in the 2M ethanol system increases significantly because of the higher uptake resulting

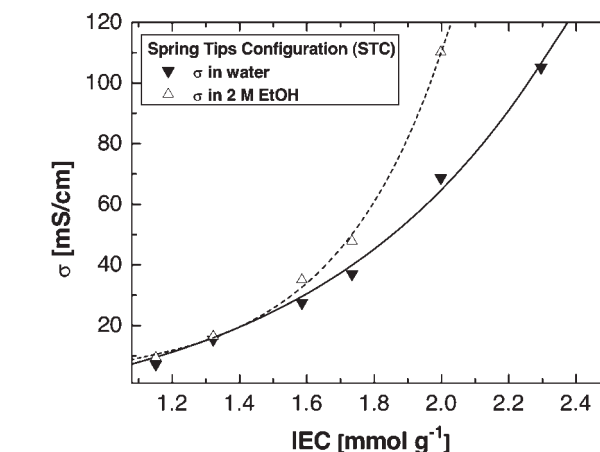


Figure 10 Proton conductivity (σ) measured with the STC in water and 2M ethanol as a function of IEC.

in excessive swelling. These results agree with the water numbers shown in Figure 8. Therefore, the water number is given as a function of IEC in Figure 11 to see how the conductivity is related to the water content in the membrane. This time, the proton conductivity measured with the PWC is given. The water number increases slightly from 8.5 to 10.2 within the IEC range of 1.1–1.6 mmol/g. The proton conductivity triples in this area from 10 to 30 mS/cm. A further increase in IEC results in an exponential increase in the water number and conductivity. In that range of IECs, membrane instability has been observed with uptake and surface area swelling. The water content in the membrane becomes higher because of the larger number of sulfonic acid groups on the polymer chains. This behavior was also found in the works of Jiang et al.⁶ and Xue and Yin,¹⁴ among others.

The proton diffusion coefficient (D_{σ}) is calculated from the proton conductivity (σ) on the basis of the Nernst–Einstein relationship:

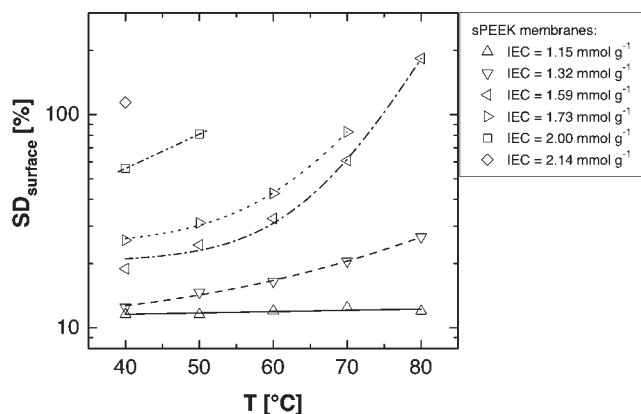


Figure 9 Membrane swelling in water as a function of temperature (T) for sPEEK membranes with various IECs.

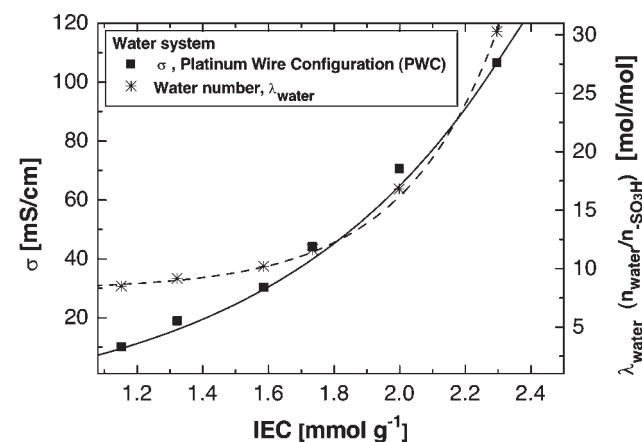


Figure 11 Proton conductivity (σ) measured with the PWC and water number (λ_{water}) as functions of IEC.

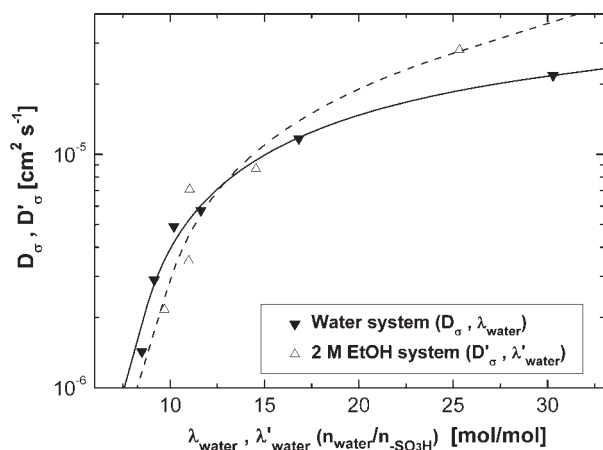


Figure 12 Proton diffusion coefficient as a function of the water number in water and 2M ethanol systems.

$$\sigma = \frac{D_{\sigma} C_{fg} F^2}{RT} \quad (11)$$

where C_{fg} is the concentration of functional groups in the membrane and is calculated with the IEC, the density of the dry membrane, and the volume swelling. F is the Faraday constant. The proton diffusion coefficient is dependent on the water content in the membrane.^{8,36,37} In Figure 12, the calculated proton diffusion coefficient is plotted against the water number. This is done for the water system (D_{σ} – λ_{water}) and the 2M ethanol system (D'_{σ} – λ'_{water}). Three different regions can be observed: (1) at $\lambda_{\text{water}} < 10$, D_{σ} is strongly dependent on λ_{water} ; (2) at $\lambda_{\text{water}} > 14$, D_{σ} is slightly dependent on λ_{water} ; and (3) at $10 < \lambda_{\text{water}} < 14$, there is a transition region. At low water numbers, the excess protons tend to be more localized in the vicinity of the sulfonic acid groups. In this region, the dissociation of the protons and the fixed anions becomes easier with the water number increasing.⁸ The dominating transport mechanism is based on the diffusion of the protons by the vehicle mechanism. In the second region, the proton diffusion coefficient is less dependent on the water number. The sulfonic acid groups are completely hydrated, and the dissociation is complete (similar to diluted acid solutions). In this region, Grotthuss hopping is the dominating transport mechanism. In Figure 12, the presence of ethanol accelerates the proton diffusion because of the larger liquid phase present in the membrane.

A transition region is around $\lambda_{\text{water}} = 12$, in which both mechanisms account for the proton transport (coupled motion). These results are in good agreement with the shift of the hydrophobicity–hydrophilicity balance and the formation of a bulky water phase observed with the uptake and surface swelling experiments. The diffusion coefficients of a

water molecule and a proton in water are 2.3×10^{-5} and 9.3×10^{-5} cm²/s, respectively.³⁸ The largest proton diffusion coefficient that we obtained was 2.2×10^{-5} cm²/s with a water number of 30. The diffusion coefficient of a proton in water was not reached, and this was also expected because of the barrier function of the membrane. The volume fractions based on wet membranes varied in our case from 0.15 to 0.55. The volume fractions were a function of IEC instead of humidity. In comparison with the literature,⁸ similar results were obtained.

Ethanol permeability

L–L systems

The permeability of ethanol and water was determined in an L–L diffusion cell. On both sides of the membrane, a liquid phase is present, and the driving force is based on the concentration difference. Permeability coefficients of water and ethanol are low in the case of low sulfonated membranes (see Fig. 13). With higher sulfonated membranes, the membrane swells excessively, and more free volume is created for the transport of both components through the membranes, so the permeabilities increase exponentially. Because of instability, it was not practicable to obtain reliable results with membranes having an IEC higher than 1.75 mmol/g.

In all cases, the water permeability coefficients exceed the ethanol permeability coefficients. However, in L–L systems, it is not possible to speak of a separation factor based on the ratio of water permeability to ethanol permeability because the transport is in opposite directions.

In Figure 14, the permeability is given as a function of the reciprocal temperature to see if the permeability shows Arrhenius behavior. Membranes with low IEC could be measured over the whole temperature interval. Membranes with an IEC of 1.6 or 1.7 mmol/g could be measured just up to a temperature of 40°C. Ethanol permeability did not show Arrhenius behavior. The increase in permeability between 25 and 40°C was relatively low in comparison with the increase in the other temperature intervals. In this temperature interval, the membrane structure is stable, and liquid transport remains low. The increase in ethanol permeability in the temperature range from 40 to 60°C is exponential, and this suggests a relationship with swelling in aqueous–ethanolic systems. This is the reason that the measurements at different temperatures do not show Arrhenius behavior. The Arrhenius equation is valid for stationary systems. The membrane swelling is dependent on the temperature. The alteration of the free volume in the membrane system results in a deviation of Arrhenius behavior.

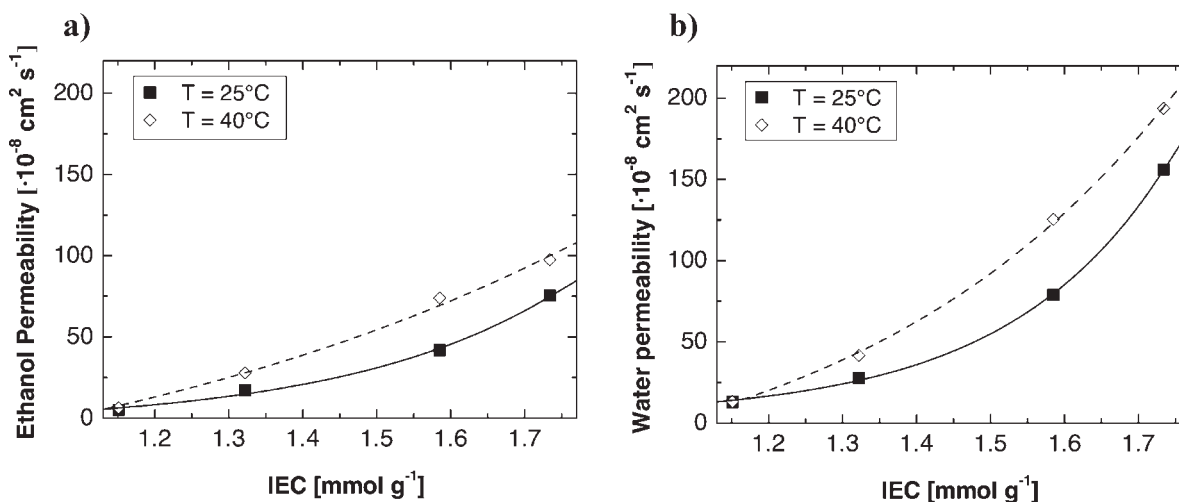


Figure 13 (a) Ethanol permeability and (b) water permeability as functions of IEC measured in a diffusion cell with an ethanol concentration difference of 4M.

L–G systems

The transport of ethanol and water through the membrane was examined in L–G systems by means of pervaporation. In the pervaporation process, this transport is in the same direction. The pervaporation results as a function of IEC are given in Figure 15. The ethanol and water flux increase exponentially with IEC, whereas the selectivity decreases. The increase in permeability accompanied by a decrease in selectivity is a well-known and unwanted feature in pervaporation processes.

The partial mass fluxes are normally expressed in $\text{g m}^{-2} \text{ h}^{-1}$.^{1,19} We prefer to use the fluxes multiplied by the membrane thickness as described in the review given by Smitha et al.³⁹ Between the measured membranes with the lowest and highest IECs, a factor of 10 in the flux increase is obtained with water, and a factor of 20 is obtained with ethanol. This means that the membrane becomes less selective when more sulfonic acid groups are present in the membrane. The hydrophilic regions in the mem-

brane grow, with the result that more water and ethanol flow through it. Remarkable are the results obtained with a membrane with an IEC of 1.3 mmol/g measured at temperatures varying from 25 to 70°C (Fig. 16). The separation factor remains constant in this temperature interval. The same observation was made by Verhoef et al.⁴⁰ The fluxes increase little in the lower temperature range (up to 50°C), and this is followed by a steep increase in the higher temperature domain. Again, Arrhenius behavior was not obtained because the swelling behavior was temperature-dependent, as shown in Figure 9. The total flux (ethanol and water) is $40 \text{ kg } \mu\text{m m}^{-2} \text{ h}^{-1}$ at 25°C and $253 \text{ kg } \mu\text{m m}^{-2} \text{ h}^{-1}$ at 70°C .

For the transport of water and isopropyl alcohol in sPEEK membranes, a model was presented by Huang et al.¹ They proposed a model in which the membrane is separated into hydrophilic and hydrophobic regions. The transport of both components is

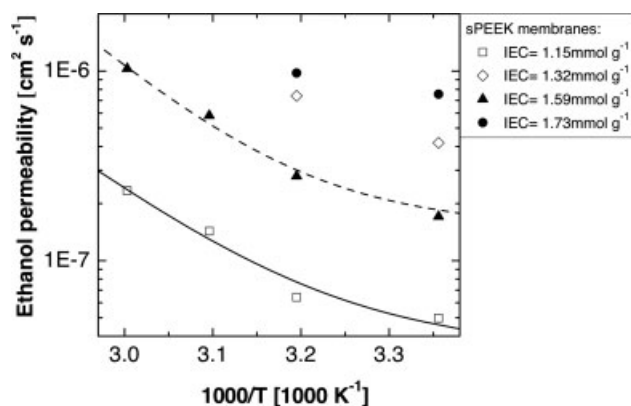


Figure 14 Arrhenius plot of the ethanol permeability for various sPEEK membranes.

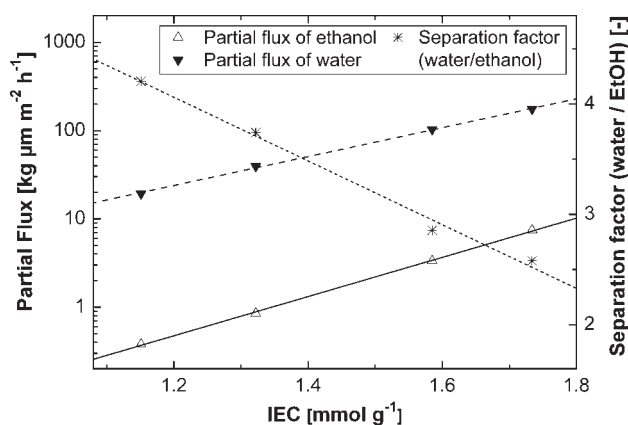


Figure 15 Partial fluxes and separation factors as functions of IEC of the sPEEK membranes (conditions: 2M ethanol feed concentration, 40°C feed temperature, and 10–15 mbar permeate pressure).

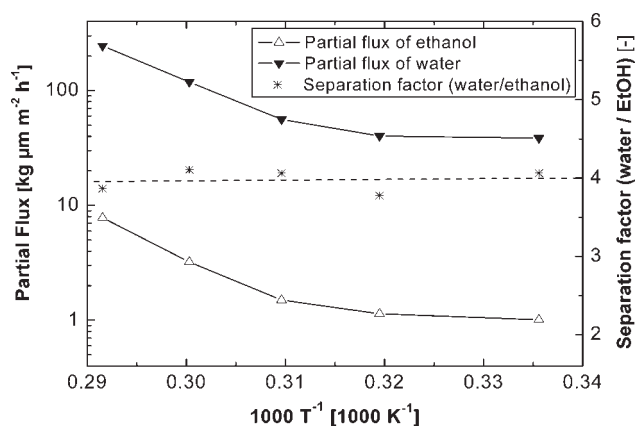


Figure 16 Temperature dependence of ethanol and water fluxes and separation factors of the sPEEK membrane with an IEC of 1.3 mmol/g (conditions: 2M ethanol feed concentration and 10–15 mbar permeate pressure).

based on a random hopping mechanism. In the case of large water uptake, the interaction between the water molecules dominates the interaction between the water molecules and sulfonic acid groups. This results in a decrease in sorption selectivity to water. The composition of the liquid in the membrane is independent of DS. They proposed that the isopropyl alcohol transport takes place because of coupled transport in the hydrophilic phase and that the transport in the hydrophobic phase can be neglected.

On the other hand, a simplified solution–diffusion model was reported by Schaetzel et al.²⁸ The model has been validated with water–ethanol pervaporation with poly(vinyl alcohol)–based membranes. The model is based on molecular diffusion. The permeant diffusivity is given as a function of the total volume occupied by all solvent species. They found that the sorption of ethanol at high water concentrations is influenced by the water present in the membrane rather than the ethanol–membrane interaction. This is similar to the findings of Huang et al.¹ The coupling effect of both components is found in the thermodynamic part (solubility). Then, the ethanol flux is only a function of the ethanol concentration gradient. The selectivity is therefore caused more by sorption and less by coupled transport.

In our case, the swelling and therefore the membrane free volume increase with increasing IEC; the sorption selectivity decreases from 2.4 to 1 in the IEC range of 1.15–1.8 mmol/g. The linear decrease in the separation factor is mainly caused by permeation of both components through hydrophilic domains of the membrane. The ethanol flux is highly dependent on the water transport in the membrane, and coupled transport takes place. This means that with ethanol–water pervaporation of a low ethanol concentration (2M ethanol), the kinetic part domi-

nates the thermodynamic part in the separation process.

sPEEK in ethanol–water systems: a comparison of L–L and L–G systems

Ethanol fluxes obtained in L–L and L–G systems are given in Figure 17 as a function of IEC. Ethanol permeability values obtained with L–L diffusion cell measurements were converted to ethanol fluxes to compare the two methods.

The ethanol flux in L–G systems increased significantly when the ethanol concentration of the feed solution was doubled from 2M to 4M. The ethanol flux measured with pervaporation was in the same direction as the water flux, and that in the diffusion cell was in the opposite direction. The increase in ethanol flux was retarded with increasing IEC in the case of the diffusion cell measurements because of the water transport in the opposite direction. The ethanol flux was enhanced in the case of pervaporation. This implies that apart from the sorption of ethanol and water in the membrane, coupled transport also takes place.

In a DEFC, the ethanol permeability should be as low as possible, whereas proton conductivity should be high. This selectivity is therefore expressed as the ratio of proton conductivity to ethanol permeability.^{14,21,41} Permeability coefficients determined in the L–L system at RT are related to the proton conductivity measured in water at RT. The selectivity as a function of IEC is given in Figure 18. sPEEK with the lowest ethanol permeability exhibited the highest selectivity. Ethanol permeability was the dominating parameter in the selectivity at RT.

As mentioned before, less attention is paid to ethanol systems than to methanol systems. For methanol, similar L–L diffusion and proton conductivity

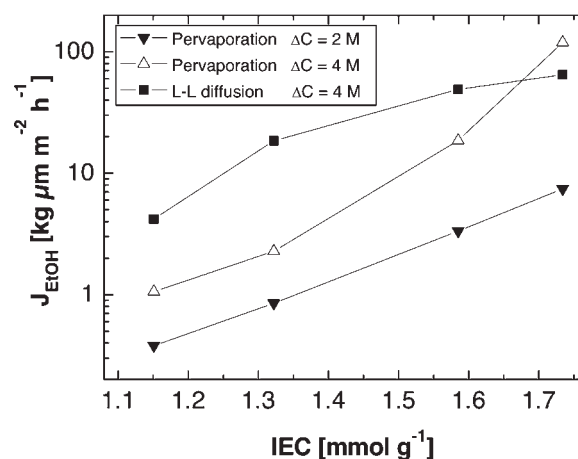


Figure 17 Comparison of the ethanol fluxes determined with different dynamic methods.

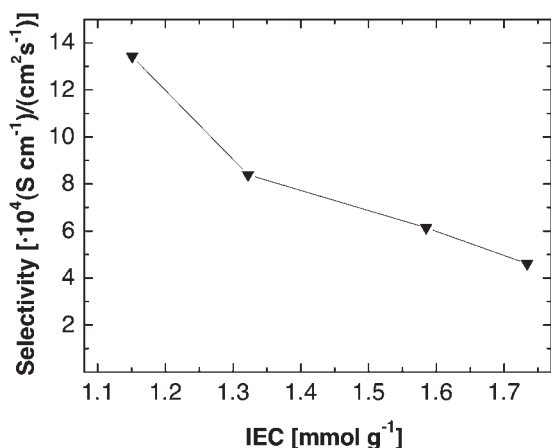


Figure 18 Selectivity (proton conductivity/permeability coefficient of ethanol) of the sPEEK membranes.

measurements are reported in the literature. Xue and Yin¹⁴ found methanol permeability coefficients as well as proton conductivity in the longitudinal direction to be a factor of 2 lower than in our systems for membranes with comparable IEC. Also, Zhong et al.⁴² found lower methanol permeability coefficients. In both cases, the methanol concentrations during the measurement were lower as well. Different swelling features occurred, and this influenced the transport. Fu et al.²¹ compared methanol and ethanol systems with modified poly(vinyl alcohol) and Nafion 117 membranes. The ethanol permeability for these membranes was lower than the permeability of methanol, except in the case of Nafion 117.

The main problem of sPEEK membranes is their instability in aqueous-ethanolic environments in relation to their proton conductivity. Low sulfonated membranes (IEC < 1.4 mmol/g) are stable, and low crossover is expected in the case of DEFC applications. The proton conductivity, however, is too low. When IEC exceeds 2 mmol/g, the membrane properties (swelling, proton conductivity, ethanol permeability, etc.) change exponentially. Because of its uncontrollable properties, the pure polymer membrane cannot be applied. According to the selectivity (proton conductivity/permeability coefficient of ethanol), the main focus lies on the reduction of the ethanol permeability. Simultaneously, the proton conductivity should be preserved or enlarged to increase the selectivity (proton conductivity/permeability coefficient of ethanol). The usage of sPEEK membranes for DEFC depends on possible modifications to stabilize the membrane in the higher conductive region rather than on modifications to increase the proton conductivity in the stable region.

CONCLUSIONS

sPEEK proton exchange membranes were prepared and characterized by their uptake, swelling behavior, proton conductivity, and ethanol permeability measurements (L-L and L-G diffusion). Uptake and swelling increased exponentially with IEC. At an IEC between 1.6 and 1.7 mmol/g, the hydrophobicity-hydrophilicity balance was shifted, and excessive swelling occurred because of a second water phase. The stability of the membranes in water at various temperatures was strongly reduced when IEC exceeded 1.6 mmol/g. This effect was even more pronounced in ethanol solutions. The proton diffusion coefficient was calculated with the measured proton conductivity. The proton transport mechanism changed around a water number of 12 from the vehicle mechanism to the Grotthuss transport mechanism. The ethanol permeability measured with a diffusion cell did not follow Arrhenius behavior. The ethanol permeability for membranes with an IEC between 1.15 and 1.75 mmol/g varied between 5×10^{-8} and 1×10^{-6} cm²/s, being dependent on the measuring temperature. Membranes with an IEC higher than 2 mmol/g could not be measured because of the lack of membrane stability. Pervaporation was measured as a function of IEC and temperature. Higher IECs accounted for higher fluxes and lower selectivity. The temperature had a large effect on the fluxes, but the selectivity remained constant. The lowest sulfonated membrane exhibited the best proton transport to ethanol permeability selectivity. The use of sPEEK membranes in DEFCs depends on possible modifications to stabilize the membrane in the higher conductive region rather than on modifications to increase the proton conductivity in the stable region.

References

- Huang, R. Y. M.; Shao, P.; Feng, X.; Burns, C. M. *J Membr Sci* 2001, 192, 115.
- Shao, P.; Huang, R. Y. M. *J Membr Sci* 2007, 287, 162.
- Sijbesma, H.; Nymeyer, K.; van Marwijk, R.; Heijboer, R.; Potreck, J.; Wessling, M. *J Membr Sci* 2008, 313, 263.
- Agmon, N. *Chem Phys Lett* 1995, 244, 456.
- Nagarale, R. K.; Gohil, G. S.; Shahi, V. K. *Adv Colloid Interface Sci* 2006, 119, 97.
- Jiang, R.; Kunz, H. R.; Fenton, J. M. *J Power Sources* 2005, 150, 120.
- Kerres, J. A. *J Membr Sci* 2001, 185, 3.
- Kreuer, K. D. *J Membr Sci* 2001, 185, 29.
- Roziere, J.; Jones, D. J. *Annu Rev Mater Sci* 2003, 33, 503.
- Jagur-Grodzinski, J. *Polym Adv Technol* 2007, 18, 785.
- Neburchilov, V.; Martin, J.; Wang, H.; Zhang, J. *J Power Sources* 2007, 169, 221.
- Li, L.; Zhang, J.; Wang, Y. *J Membr Sci* 2003, 226, 159.
- Xing, P.; Robertson, G. P.; Guiver, M. D.; Mikhailenko, S. D.; Wang, K.; Kaliaguine, S. *J Membr Sci* 2004, 229, 95.
- Xue, S.; Yin, G. *Eur Polym J* 2006, 42, 776.

15. Nagarale, R. K.; Gohil, G. S.; Shahi, V. K. *J Membr Sci* 2006, 280, 389.
16. Wang, J.; Yue, Z.; Economy, J. *J Membr Sci* 2007, 291, 210.
17. Gaowen, Z.; Zhentao, Z. *J Membr Sci* 2005, 261, 107.
18. Karthikeyan, C. S.; Nunes, S. P.; Prado, L. A. S. A.; Ponce, M. L.; Silva, H.; Ruffmann, B.; Schulte, K. *J Membr Sci* 2005, 254, 139.
19. Nunes, S. P.; Ruffmann, B.; Rikowski, E.; Vetter, S.; Richau, K. *J Membr Sci* 2002, 203, 215.
20. Zaidi, S. M. J.; Ahmad, M. I. *J Membr Sci* 2006, 279, 548.
21. Fu, R.-Q.; Hong, L.; Lee, J. Y. *Fuel Cells* 2008, 8, 52.
22. Tan, A. R.; Carvalho, L. M. D.; Filho, F. G. D. R.; Gomes, A. D. S. *Macromol Symp* 2006, 245, 470.
23. Huang, R. Y. M.; Shao, P.; Burns, C. M.; Feng, X. *J Appl Polym Sci* 2001, 82, 2651.
24. Robertson, G. P.; Mikhailenko, S. D.; Wang, K.; Xing, P.; Guiver, M. D.; Kaliaguine, S. *J Membr Sci* 2003, 219, 113.
25. Wilhelm, F. G.; Pünt, I. G. M.; Vegt, N. F. A. V. D.; Strathmann, H.; Wessling, M. *J Membr Sci* 2002, 199, 167.
26. Nolte, R.; Ledjeff, K.; Bauer, M.; Mulhaupt, R. *J Membr Sci* 1993, 83, 211.
27. Wu, H.-L.; Ma, C.-C. M.; Liu, F.-Y.; Chen, C.-Y.; Lee, S.-J.; Chiang, C.-L. *Eur Polym J* 2006, 42, 1688.
28. Schaetzel, P.; Vauclair, C.; Nguyen, Q. T.; Bouzerar, R. *J Membr Sci* 2004, 244, 117.
29. Smits, F. M. *Bell Syst Tech J* 1958, 37, 711.
30. Benjamin, M. C.; Hillard, R. J.; Borland, J. O. *Nucl Instrum Methods Phys Res Sect B* 2005, 237, 351.
31. Cahan, B. D.; Wainright, J. S. *J Electrochem Soc* 1993, 140, L185.
32. Zawodzinski, T. A.; Neeman, M.; Sillerud, L.; Cottesfeld, S. *J Phys Chem* 1991, 95, 6040.
33. Kaliaguine, S.; Mikhailenko, S. D.; Wang, K. P.; Xing, P.; Robertson, G.; Guiver, M. *Catal Today* 2003, 82, 213.
34. Li, X.; Zhao, C.; Lu, H.; Wang, Z.; Na, H. *Polymer* 2005, 46, 5820.
35. Kreuer, K. D. *Solid State Ionics* 1997, 97, 1.
36. Wu, H.-L.; Ma, C.-C. M.; Li, C.-H.; Lee, T.-M.; Chen, C.-Y.; Chiang, C.-L.; Wu, C. *J Membr Sci* 2006, 280, 501.
37. Cano-Serrano, E.; Campos-Martin, J. M.; Fierro, J. L. G. *Chem Commun* 2003, 246.
38. Atkins, P. W. *Physical Chemistry*; Oxford University Press: Oxford, 1994.
39. Smitha, B.; Suhanya, D.; Sridhar, S.; Ramakrishna, M. *J Membr Sci* 2004, 241, 1.
40. Verhoef, A.; Figoli, A.; Leen, B.; Bettens, B.; Drioli, E.; Van der Bruggen, B. *Sep Purif Technol* 2008, 60, 54.
41. Pivovar, B. S.; Wang, Y.; Cussler, E. L. *J Membr Sci* 1999, 154, 155.
42. Zhong, S.; Cui, X.; Cai, H.; Fu, T.; Zhao, C.; Na, H. *J Power Sources* 2007, 164, 65.